

Comparison of quantum kinetic theory and time-dependent Dirac equation approaches in vacuum pair production and the bound states resonance enhanced mechanism

Q. Wang,¹ L. B. Fu,^{2,3,*} and J. Liu^{1,3}

¹*Institute of Applied Physics and Computational Mathematics, Beijing 100088, China*

²*Graduate School, China Academy of Engineering Physics, Beijing 100193, China*

³*HEDPS, Center for Applied Physics and Technology, Peking University, Beijing 100871, China and CICIFSA MoE College of Engineering, Peking University, Beijing 100871, China*

A remarkable quantitative agreement is found between the non-Markovian quantum kinetic approach and the time-dependent Dirac equation approach for a large region of Keldysh parameter, in the investigation of electron-positron pair production in the electric fields which is spatially homogeneous and envelope pulse shaped. If a sub-critical bound potential is immersed in this background field, the TDDE results show that the creation probability will be enhanced by the bound states resonance by two orders of magnitude. We also establish a computing resources greatly saved TDDE formalism for spatially homogeneous field.

PACS numbers: 12.20.Ds, 11.15.Tk, 25.75.Dw, 52.25.Dg

Introduction. In the presence of a very strong electric field the quantum electrodynamics (QED) vacuum may break down and decay via the production of electron-positron pairs. This effect was first discussed by Sauter[1] and computed by Schwinger for the spatially homogeneous and static electric fields[2]. Since then various theoretical techniques were developed to deal with more complicate field configurations[3].

In recent years, the quantum kinetic theory (QKT) based on Vlasov equations including a source term was established to resolve the dynamics of the production process which is in general non-equilibrium and time-dependent [4, 5]. QKT is rigorously derived from QED by canonical quantization of the Dirac field and subsequently Bogoliubov transformation to a quasi-particle representation. It is exact on the mean-field level. In the sub-critical field strength regime, the collision [6, 7] and back reaction[7–9] terms can be neglected safely. It is easily to implement numerical calculation, and can provide not only the pair production rate but also the momentum distribution information. These advantages make it a powerful tool to investigate pair creation in complicated temporal field configurations[10, 11]. QKT has been proved to be equivalent to the DHW formalism in the case of linearly polarized electric fields[12], and to the scattering approach[13]. One the other hand, the disadvantage of QKT is obvious that its application is restricted to spatial homogeneous field, thus to one dimension.

In a realistic experiment, the spatial variation of the field should be taken into account. In current literature, the electron-positron pair number can be obtained by the time-dependent Dirac equation approach (TDDE). Pair production in laser fields oscillating in space and time is investigated by propagating an initially negative-energy Gaussian wave packet in the spatial- and temporal- dependent fields and projecting it onto positive energy states after the fields has been turned off [14]. This ap-

proach based on one-particle time-dependent Dirac equation has rigorous foundation in the well-established revised version of Furry's formulation of QED in external fields with unstable vacuum[15–17]. Another approach is the called numerical quantum field theory method, where the pair number is obtained by propagating all the negative energy states in the time dependent Dirac Hamiltonian and projecting them over all positive energy states [18]. In the following, the abbreviation 'TDDE' denotes the later. In contrast to QKT, in TDDE approach the spatial variation of the field can be taken into account, and the information of spatial and momentum distribution of both electrons and positrons can be computed easily as well. In principle, if applied in homogeneous fields, the TDDE approach must be equivalent to QKT. However, surprisingly, few works have been done to examine this equivalence. This will be the first goal of this paper.

In a recent work[19], it is suggested that if additional binding potentials (like that of a bare nucleus) are immersed in the constant electric field region, the corresponding bound state can enhance the pair creation. Of course, similar to the charge resonance enhanced ionization of molecular physics[20–22], bound states (for example, supported by a super strong nuclear Coulomb field characteristic of two colliding high-Z ions) play an important role in the pair creation process. In the work[23], where bound states located in the gap supported by the well potential are exposed in an oscillating electric field, an simple matchup between bound states and momentum distribution was found. The second goal of the letter is, in a real binding potential, examining the bound states enhanced pair creation using the TDDE approach.

In the following, we will first briefly review the two approaches, and establish a formalism for TDDE in spatial homogeneous case. The natural units are used, that $\hbar = e = c = 1$ with other quantities scaled by m . Then, for a homogeneous time-dependent electric field pulse, we

compare and discuss the numerical results. Finally we show the bound states resonance enhanced pair creation.

Quantum Kinetic Theory approach (QKT).

Assuming the vector potential is $\mathbf{A} = (0, 0, A_z(t))$, since momentum $\mathbf{k}(k_\perp, k_z)$ is a good quantum number, the field operator $\hat{\Phi}(\mathbf{x}, t)$ is decomposed as $\hat{\Phi}(\mathbf{x}, t) = \int d\mathbf{k} e^{i\mathbf{k}\cdot\mathbf{x}} \left(u_{\mathbf{k}}(t) \tilde{a}_{\mathbf{k}} + u_{\mathbf{k}}^*(t) \tilde{b}_{-\mathbf{k}}^\dagger \right)$, where $\tilde{a}_{\mathbf{k}}$ and $\tilde{b}_{-\mathbf{k}}^\dagger$ correspond to the annihilation (creation) operators for the particle and the antiparticle respectively with the momentum $|\mathbf{k}|$. The transformation between time dependent operators $(a_{\mathbf{k}}(t), b_{\mathbf{k}}(t))$ and time independent operators $(\tilde{a}_{\mathbf{k}}, \tilde{b}_{\mathbf{k}})$ is expressed in terms of the Bogoliubov coefficients $\alpha_{\mathbf{k}}(t)$ and $\beta_{\mathbf{k}}(t)$,

$$a_{\mathbf{k}}(t) = \alpha_{\mathbf{k}}(t) \tilde{a}_{\mathbf{k}} - \beta_{\mathbf{k}}^*(t) \tilde{b}_{-\mathbf{k}}^\dagger, \quad (1)$$

$$b_{-\mathbf{k}}^\dagger(t) = \beta_{\mathbf{k}}(t) \tilde{a}_{\mathbf{k}} + \alpha_{\mathbf{k}}^*(t) \tilde{b}_{-\mathbf{k}}^\dagger, \quad (2)$$

with $|\alpha_{\mathbf{k}}(t)|^2 + |\beta_{\mathbf{k}}(t)|^2 = 1$. By making an adiabatic ansatz for $u_{\mathbf{k}}(t)$ [13], the Dirac equation which $\hat{\Phi}(\mathbf{x}, t)$ obeys reduces to an oscillator equation $\ddot{u}_{\mathbf{k}}(t) + \left(\omega^2(\mathbf{k}, t) + i\dot{P}_z(t) \right) u_{\mathbf{k}}(t) = 0$, where $\omega^2(\mathbf{k}, t) = m^2 + k_\perp^2 + P_z^2$, $P_z(t) = k_z + A_z(t)$. The number of pairs for each \mathbf{k} is defined as $N(\mathbf{k}, t) = |\beta_{\mathbf{k}}(t)|^2$. The adiabatic ansatz gives the creation rate as the source term of the quantum Vlasov equation, $\dot{N}(\mathbf{k}, t) = W(\mathbf{k}, t) \int_{-\infty}^t W(\mathbf{k}, t') (1 - N(\mathbf{k}, t')) \cos\left(2 \int_t^{t'} \omega(\mathbf{k}, \tau) d\tau\right) dt'$, where $W(\mathbf{k}, t) = \frac{eE_z(t)\epsilon_\perp(t)}{\omega^2(\mathbf{k}, t)}$, $\epsilon_\perp^2(t) = k_\perp^2 + m^2$, $E(t)$ is the electric field along z direction $E_z(t) = -\dot{A}_z(t)$, and $P_z(t)$ denotes the time-dependent kinetic momentum. For computational efficiency, by introducing two auxiliary functions $G(\mathbf{k}, t)$ and $H(\mathbf{k}, t)$, the quantum Vlasov equation can be re-expressed as first-order differential equations[8],

$$\dot{N}(\mathbf{k}, t) = W(\mathbf{k}, t) G(\mathbf{k}, t), \quad (3)$$

$$\dot{G}(\mathbf{k}, t) = W(\mathbf{k}, t) [1 - N(\mathbf{k}, t)] - 2\omega(\mathbf{k}, t) H(\mathbf{k}, t), \quad (4)$$

$$\dot{H}(\mathbf{k}, t) = 2\omega(\mathbf{k}, t) G(\mathbf{k}, t), \quad (5)$$

with initial conditions $N(\mathbf{k}, -\infty) = G(\mathbf{k}, -\infty) = H(\mathbf{k}, -\infty) = 0$. Here N accounts for both spin directions. These equations can be solved easily using Runge-Kutta methods. Throughout the article, we perform all simulations in one dimension, $k_\perp = 0$. Then the particle yield per Compton wavelength (λ_C) reads $N = \int dk_z / (2\pi) N(k_z, +\infty)$.

Time-dependent Dirac Equation (TDDE).

Here the field operator $\hat{\Psi}(\vec{\mathbf{x}}, t)$ is also expressed in terms of the electron annihilation \hat{b} and positron creation \hat{d}^\dagger operators, $\hat{\Psi}(\vec{\mathbf{x}}, t) = \sum_p \hat{b}_p \varphi_p(\vec{\mathbf{x}}, t) + \sum_n \hat{d}_n^\dagger \varphi_n(\vec{\mathbf{x}}, t)$, and the relations between the time dependent and time independent operator are,

$$\hat{b}_p(t) = \sum_{p'} \hat{b}_{p'} U_{pp'}(t) + \sum_{n'} \hat{d}_{n'}^\dagger U_{pn'}(t), \quad (6)$$

$$\hat{d}_n^\dagger(t) = \sum_{p'} \hat{b}_{p'} U_{np'}(t) + \sum_{n'} \hat{d}_{n'}^\dagger U_{nn'}(t). \quad (7)$$

Particle information can be obtained from the field operator, e.g., the spacial distribution of electrons created from the vacuum (defined as $\hat{b}_p \|vac\rangle = 0$, $\hat{d}_n \|vac\rangle = 0$) is obtained from the positive part of the field operator, $N^{el.}(\vec{\mathbf{x}}, t) = \langle vac \| \hat{\Psi}^{(+)\dagger}(x, t) \hat{\Psi}^{(+)}(x, t) \| vac \rangle$. The pair number reads, $N(t) = \sum_{pn} |U_{pn}(t)|^2$. The density and momentum distribution of electrons are $N^{el.}(\vec{\mathbf{x}}, t) = \sum_n \left| \sum_p U_{pn}(t) \varphi_p(\vec{\mathbf{x}}) \right|^2$, $N^{el.}(p, t) = \sum_n |U_{pn}(t)|^2$. These quantities of positrons can also be computed, $N^{po.}(\vec{\mathbf{x}}, t) = \sum_p \left| \sum_n U_{pn}(t) \varphi_n(\vec{\mathbf{x}}) \right|^2$, $N^{po.}(n, t) = \sum_p |U_{pn}(t)|^2$. Here the transition probability $U_{pn}(t) = \int d\vec{\mathbf{x}} \varphi_p^*(\vec{\mathbf{x}}) \varphi_n(\vec{\mathbf{x}}, t)$ is computed by propagating every initial negative energy eigen-states by spatial- and temporal- dependent Dirac Hamiltonian, and then projecting them over all positive energy eigen-states. $\sum_{p(n)}$ denote the summation over all states with positive (negative) energy. $\varphi_{p(n)}(\vec{\mathbf{x}})$ are the positive (negative) energy eigen-states of the field-free Dirac Hamiltonian, $\varphi_{p(n)}(\vec{\mathbf{x}}, t)$ are solutions of the time dependent Dirac equation with potential taking into account, $\varphi_{p(n)}(\vec{\mathbf{x}}, t) = \hat{U}(t, -\infty) \varphi_{p(n)}(\vec{\mathbf{x}})$, and can be obtained using the numerical split operator technique[24]. The time-evolution operator is defined as $\hat{U}(t_2, t_1) = \hat{T} \exp\left(-i \int_{t_1}^{t_2} dt' \hat{H}(t')\right)$, where \hat{T} denotes the Dyson time ordering operator. The Dirac Hamiltonian is $H = \boldsymbol{\alpha} \cdot \mathbf{p} + m\beta - A_0 + \boldsymbol{\alpha} \cdot \vec{A}$, where A_0 and \vec{A} denote scalar and vector potentials, $\vec{E} = -\nabla A_0 - \dot{\vec{A}}$. Each temporal step reads $\varphi(\vec{\mathbf{x}}, t + dt) \approx \exp\left(-i \frac{dt}{2} H_\partial\right) \exp(-idt H_{\vec{\mathbf{x}}}) \exp\left(-i \frac{dt}{2} H_\partial\right) \varphi(\vec{\mathbf{x}}, t) + O(dt^3)$, where $H_\partial = \boldsymbol{\alpha} \cdot \mathbf{p} + m\beta$ and $H_{\vec{\mathbf{x}}} = -A_0 + \boldsymbol{\alpha} \cdot \vec{A}$ are implemented in momentum and coordinate space respectively.

Generally, in one dimension one choose the gauge $A_0 = A_0(z, t)$, $\vec{A} = (0, 0, 0)$ to describe the spatial and temporal dependent electric field. However, in the case of spatial homogeneous field, $A_0(z, t)$ is linearly depend on space. This also introduce a spatial dependent variable to the simulation, and bring errors. So we choose gauge $A_0 = 0$, $\vec{A} = (0, 0, A_z(t))$ to make H only temporal dependent. In this work, since the field makes the spin invariant and it is sufficient to focus on the spinless state in the discussion followed, Dirac matrix in H are reduced to Pauli matrix. The Hamiltonian is $H = \sigma^1(p_z + A_z(t)) + m\sigma^3$. The splitting can be done in two equivalent forms: (a) $H_\partial = \sigma^1 p_z + m\sigma^3$, $H_z = \sigma^1 A_z(t)$, (b) $H_\partial = \sigma^1(p_z + A_z(t)) + m\sigma^3$, $H_z = 0$.

Until now, the eigen-states are expressed and the propagating are done in coordinate space. The pair yield here is an extensive quantity corresponding to numerical box L . To compare with the QKT results, it should be converted into an intensive quantity, i.e., pair yield per Compton wavelength (λ_C). The pair number should also multiply two for the spin degeneracy.

To reduce the computational cost, in the spatial homogeneous case, we choose split (b). Then

$$\exp(-idtH_\partial) = \mathcal{F}^{-1} \{ \Gamma(t) \} \mathcal{F}, \quad (8)$$

$$\exp(-idtH_z) = I, \quad (9)$$

$$\Gamma(t) \equiv \cos(\phi) - idt \sin(\phi) \frac{\sigma^3 m + \sigma^1 P_z(t)}{\phi}, \quad (10)$$

where $\phi = dt\sqrt{m^2 + P_z(t)^2}$, $P_z(t) = k_z + A(t)$, I is unit matrix, and $\mathcal{F}^{-1}(\mathcal{F})$ denotes (inverse) Fourier transformation. Then the evolution of each temporal step actually can be done only in momentum space. Using the orthogonality of the eigen-states, $U_{pn}(t)$ is diagonal. The pair number reads $N(t) = \sum_k |U_k(t, t_0)|^2$, and

$$U_k(t, t_0) = [u_{k,a}^* \ u_{k,b}^*] \Gamma(t) \dots \Gamma(t_0 + dt) \Gamma(t_0) \begin{bmatrix} v_{k,a} \\ v_{k,b} \end{bmatrix} \quad (11)$$

where $t_0 \rightarrow -\infty$, $u_{k,a(b)}$ and $v_{k,a(b)}$ denote the coefficients of the solutions $u_k(z)$ and $v_k(z)$ of field free Dirac Hamiltonian $H = \sigma^1 p_z + m\sigma^3$, $u_k(z) = e^{ipz} [u_{k,a} \ u_{k,b}]^T$ for positive solutions and $v_k(z) = e^{ikz} [v_{k,a} \ v_{k,b}]^T$ for negative solutions. $u_{k,a} = \frac{\sqrt{E_k + m}}{\sqrt{4\pi E_k}}$, $u_{k,b} = \frac{\text{sgn}(k) \sqrt{E_k - m}}{\sqrt{4\pi E_k}}$, $v_{k,a} = -\text{sgn}(k) \frac{\sqrt{E_k - m}}{\sqrt{4\pi E_k}}$, $v_{k,b} = \frac{\sqrt{E_k + m}}{\sqrt{4\pi E_k}}$, $E_k = \sqrt{m^2 + k^2}$. $\Gamma(t)$ is a 2×2 matrix whose every element is an function of canonical momentum k . Now because the transition probability $U_{pn}(t)$ is diagonal, Eq. (6) and (7) degenerate to Eq. (1) and (2) respectively. This is a convincing evidence of the equivalence between these two approaches.

Numerical results.

The equivalence. We consider a spacial homogeneous electric pulse of the form $\vec{E}(t) = (0, 0, E_z(t))$,

$$E_z(t) = \varepsilon \exp\left(\frac{-t^2}{2\tau^2}\right) \cos(\omega t), \quad (12)$$

with peak strength ε , duration τ and frequency ω . We choose pulse duration $\tau = 20/m$ and peak strength $\varepsilon = 0.01, 0.1, 1m^2$. The numerical results are shown in Fig.1. The results have rich physics. For $\varepsilon = 0.01, 0.1$, the final pair yield $N(t \rightarrow +\infty)$ exhibits a oscillatory structure which is a signature of multiphoton production.

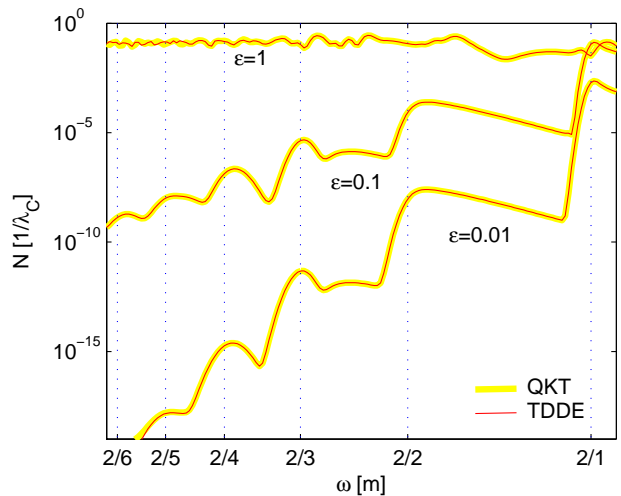


Figure 1. Particle yields per Compton wavelength (λ_C) as a function of frequency ω computed by QKT and TDDE coincide exactly. The dashed line indicate the thresholds $2/n$, where n is the photon number.

Its thresholds are $n\omega = 2m$ (dashed lines in Fig.1, n is the photon number, $2m$ is the mass gap). In this log-log diagram, the linear decay of the pair yield at thresholds as frequency vanishing indicate a power law decay. Since $N \sim \varepsilon^{2n}$, peaks at $2m/n$ on curve $\varepsilon = 0.01$ are $2n$ orders smaller than on curve $\varepsilon = 0.1$. Due to the finite duration τ , the multiphoton peaks are not sharp. The slightly deviation of the peaks above $2m/n$ is a signature of the effective mass of the particles in strong field[11]. If the field is strong enough, e.g., $\varepsilon = 1$, the mechanism of pair production get in the tunneling region, and the multiphoton peaks disappear. Of course, here the collision and back reaction are neglected. As the results shown, for weak and strong field, namely a large region of Keldysh parameter, the two approaches coincide exactly.

In order to get more deep insight, we plot the energy distribution for $\varepsilon = 0.1$, $\omega = 0.5, 1, 2m$ in Fig.2, corresponding to four, two and one photon resonance respectively. In the sub-figure (a), in addition to the main peak at $E = 1$ (zero momentum) which is due to 4-photon absorption, peaks arise due to the absorption of s additional photons. Since $(n+s)\omega = 2E$ (E is the energy of single electron, $n = 4$, $\omega = 0.5m$), the peaks arise at $E = (1+s/4)m$. For lower energy, the two approaches coincide exactly, even at the peak $s = 1$ which is split. However, QKT fail to describe higher energy excitation due to the approximation[13] used in its derivation. On the other hand, TDDE approach with no approximation used can provide more accuracy and capture the physics of higher order multiphoton absorption though it contribute little for the total pair yield. The high frequency irregular oscillation at the magnitude of $\sim 10^{-30}$ is the limit of precision of TDDE simulation.

Bound states resonance enhanced pair cre-

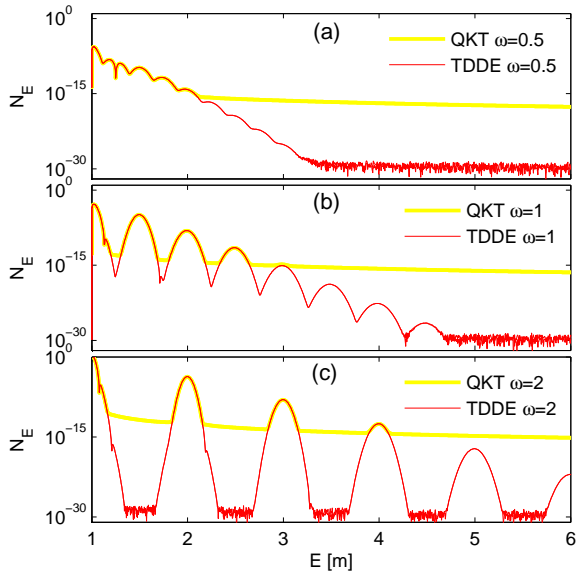


Figure 2. The energy distribution for $\epsilon = 0.1$, $\omega = 0.5, 1, 2m$.

ation.

Now let's turn to the immersed bound states enhanced pair creation. The spacial homogeneous back ground field takes the form as Eq. (12). The bound states are supported by a Sauter-like well potential, $V = -A_0$, $\vec{A} = (0, 0, 0)$,

$$V(z) = \frac{V_0}{2} \left[\tanh\left(\frac{z - W/2}{D}\right) - \tanh\left(\frac{z + W/2}{D}\right) \right], \quad (13)$$

where D is the extension of each edge, W is the total width. We set $D = 0.3\lambda_C$ and $W = 4\lambda_C$. For $V_0 = 1m$, in the well there are bound states of energy $E_b = 0.19, 0.58m$, and for $V_0 = 0.8m$, $E_b = 0.37, 0.73m$. To avoid time effect[25], $V(z)$ is turned on with a modulation coefficient $f(t + T/2)$, $f(t) = \sin^2(\pi t/2t_1)$. When $t \in [-T/2 + t_1, T/2 - t_1]$, $f(t) = 1$, that means $V(z)$ is holding on in this time region. Finally, $V(z)$ is turned off in the way $f(t - (T/2 - t_1))$, $f(t) = \cos^2(\pi t/2t_1)$. Here T is total pulse duration. We choose $T = 16\tau$ and $t_1 = \tau$, $\tau = 20/m$ is the pulse duration of Eq. (12).

If there is only well potential exist, the final pair yield produced is zero because here it is sub-critical. (Numerically, using TDDE, the particle yield $< 10^{-9}$). The spacial homogeneous electric pulse, Eq. (12) with $\epsilon = 0.1m^2$, can produce pairs, as black line in Fig.3, see also Fig.1. Immersing the well potential in the center of the spacial homogeneous field of length $L = 137\lambda_C$, particle yields as a function of ω computed by TDDE are shown as red and green lines in Fig.3. The vertical fine line indicate $\omega = E_b - (-m)$ for the two well respectively. $-m$ is the Dirac sea level. The results clearly shown that when the photon energy equal to the distance between

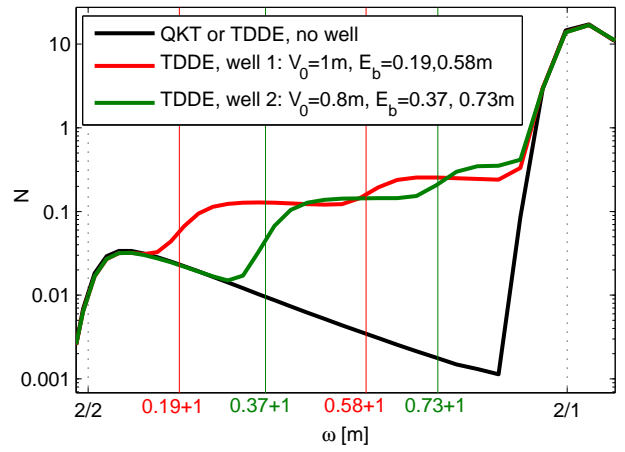


Figure 3. Particle yields as a function of frequency ω computed by TDDE when the well potential is immersed in the homogeneous back ground field (red and green lines). The back ground field takes the form Eq. (12) with $\tau = 20/m$, $\epsilon = 0.1m^2$, and its particle yields is also shown here (black line) for comparison. The well potential takes the form Eq. (13) with $D = 0.3\lambda_C$, $W = 4\lambda_C$ and the turning on and turning off duration $t_1 = \tau$. The total duration is $T = 16\tau$. The length of numerical box is $L = 137\lambda_C$.

bound state and Dirac sea level, pair creation process is enhanced. The largest enhancement is 2 orders of magnitude for a typical length scale $L = 137\lambda_C$. The pair yield can be decomposed of two parts. One is produced by the background field, and the other by bound states resonance enhancement. Additionally simulation show that, at fixed ω if we increase L , the first part increases linearly, and the second part remains constant. For $V_0 = 1m$, the max enhancement $\max(N_{enhance}) = 0.25$ occurs at $\omega = 1.7m$, and for $V_0 = 0.8m$, it is $\max(N_{enhance}) = 0.35$ at $\omega = 1.85m$. In the region far away from the resonance, the well potential do not change the pair yield.

Summary. We have demonstrated that the two widely used approaches are equivalent. For a homogeneous electric pulse, the particle yield coincide exactly in a large field strength and frequency region, from the photon absorption region to the non-perturbative tunneling region, except that the QKT fails to describe higher energy excitation and provides less accuracy than TDDE. The details of the approximation of QKT is left to study in future work. Using TDDE, we studied the bound states enhanced pair production by immersing bound states into homogeneous time-dependent back-ground field. For a typical length scale $L = 137\lambda_C$, the largest enhancement here is 2 orders of magnitude, in spite of that two fields are all sub-critical. This result is helpful for future experiment design.

Furthermore, due to TDDE's huge computational cost of propagating all negative energy states in time, only one dimensional system has been studied until now. In work[26], for spatial dependent case, we neglect the larger

part of the discrete momentum to reduce computational cost. In this work, for spatial homogeneous case, we established a formalism which greatly save computing resources. For example, in Fig.2, the simulation of TDDE takes only 2 seconds using matlab on a personal stand-alone computer, even more faster than the 10 seconds of QKT. This makes it possible that TDDE can be used to study higher dimensional systems in which more exciting physics exist. Finally, all discussion in this paper focus on Fermions described by Dirac equation. The generation to Bosons described by Klein-Gordon equation is directly.

This work is supported by the National Basic Research Program of China (Contracts No. 2013CB834100) and the National Natural Science Foundation of China (Contracts No. 11274051, No. 11374040, No. 11475027, and No. 11575027).

* lbfu@iapcm.ac.cn

- [1] F. Sauter, *Z. Phys.* **69**, 742 (1931).
- [2] J. Schwinger, *Phys. Rev.* **82**, 664 (1951).
- [3] E. Brézin and C. Itzykson, *Phys. Rev. D* **2**, 1191 (1970); V. S. Popov, *Zh. Eksp. Teor. Fiz.* **61**, 1334 (1971) [*Sov. Phys. JETP* **34**, 709 (1972)]; **62**, 1248 (1972) [*Sov. Phys. JETP* **35**, 659 (1972)]; V. G. Bagrov, D. M. Gitman, S. P. Gavrilov, and Sh. M. Shvartsman, *Izv. Vuz. Fiz.* **3**, 71 (1975) [*Sov. Phys. J.* **18**, 351 (1975)]; M. S. Marinov and V. S. Popov, *Fortschr. Phys.* **25**, 373 (1977); Y. Kluger, J.M. Eisenberg, B. Svetitsky, F. Cooper, and E. Mottola, *Phys. Rev. Lett.* **67**, 2427 (1991); *Phys. Rev. D* **45**, 4659 (1992); S. P. Gavrilov and D. M. Gitman, *Phys. Rev. D* **53**, 7162 (1996); Y. Kluger, E. Mottola, and J. M. Eisenberg, *Phys. Rev. D* **58**, 125015 (1998); S. P. Kim and D. N. Page, *Phys. Rev. D* **65**, 105002 (2002); **73**, 065020 (2006); **75**, 045013 (2007). A. Di Piazza, *Phys. Rev. D* **70**, 053013 (2004); H. Gies and K. Klingmüller, *Phys. Rev. D* **72**, 065001 (2005); G. V. Dunne and C. Schubert, *Phys. Rev. D* **72**, 105004 (2005); G. V. Dunne, Q.-h. Wang, H. Gies, and C. Schubert, *Phys. Rev. D* **73**, 065028 (2006); C. K. Dumlu and G. V. Dunne, *Phys. Rev. Lett.* **104**, 250402 (2010); *Phys. Rev. D* **83**, 065028 (2011).
- [4] S. A. Smolyansky, G. Röpke, S. Schmidt, D. Blaschke, V. D. Toneev, and A. V. Prozorkevich, arXiv:hep-ph/9712377; S. Schmidt, D. Blaschke, G. Röpke, S. Smolyansky, A. Prozorkevich, and V. Toneev, *Int. J. Mod. Phys. E* **07**, 709 (1998).
- [5] Y. Kluger, E. Mottola, and J. M. Eisenberg, *Phys. Rev. D* **58**, 125015 (1998);
- [6] D. V. Vinnik, et al., *Eur. Phys. J. C* **22**, 341 (2001);
- [7] N. Tanji, *Annals Phys.* **324**, 1691 (2009) .
- [8] J. C. Bloch, V. A. Mizerny, A. V. Prozorkevich, C. D. Roberts, S. M. Schmidt, S. A. Smolyansky, and D. V. Vinnik, *Phys. Rev. D* **60**, 116011 (1999).
- [9] C. D. Roberts, S.M. Schmidt, *Prog. Part. Nucl. Phys.* **45**, S1 (2000).
- [10] S. Schmidt, D. Blaschke, G. Röpke, A. V. Prozorkevich, S. A. Smolyansky, and V. D. Toneev, *Phys. Rev. D* **59**, 094005 (1999); R. Alkofer, M. B. Hecht, C. D. Roberts, S. M. Schmidt, and D. V. Vinnik, *Phys. Rev. Lett.* **87**, 193902 (2001); C. D. Roberts, S. M. Schmidt, and D. V. Vinnik, *Phys. Rev. Lett.* **89**, 153901 (2002); D. B. Blaschke, A. V. Prozorkevich, C. D. Roberts, S. M. Schmidt, S. A. Smolyansky, *Phys. Rev. Lett.* **96**, 140402 (2006); F. Hebenstreit, R. Alkofer, and H. Gies, *Phys. Rev. D* **78**, 061701 (2008); F. Hebenstreit, R. Alkofer, G. V. Dunne, and H. Gies, *Phys. Rev. Lett.* **102**, 150404 (2009); M. Orthaber, F. Hebenstreit, and R. Alkofer, *Phys. Lett. B* **698**, 80 (2011).
- [11] C. Kohlfürst, H. Gies and R. Alkofer, *Phys. Rev. Lett.* **112**, 050402 (2014).
- [12] I. Bialynicki-Birula, P. Gornicki, and J. Rafelski, *Phys. Rev. D* **44**, 1825 (1991). F. Hebenstreit, Ph.D. thesis, University of Graz, 2011; F. Hebenstreit, R. Alkofer, and H. Gies, *Phys. Rev. D* **82**, 105026 (2010); A. Blinne and E. Strobel, *Phys. Rev. D* **93**, 025014 (2016).
- [13] C. K. Dumlu, *Phys. Rev. D* **79**, 065027 (2009). A. M. Fedotov, E. G. Gelfer, K. Yu. Korolev, and S. A. Smolyansky, *Phys. Rev. D* **83**, 025011 (2011).
- [14] M. Ruf, G. R. Mocken, C. Müller, K. Z. Hatsagortsyan, and C. H. Keitel, *Phys. Rev. Lett.* **102**, 080402 (2009); G. R. Mocken, M. Ruf, C. Müller, and C. H. Keitel, *Phys. Rev. A* **81**, 022122 (2010).
- [15] M. Ruf, Ph.D. dissertation, Max Planck Institute for Nuclear Physics, 2009.
- [16] E. S. Fradkin, D. M. Gitman, and S. M. Shvartsman, *Quantum-Electrodynamics with unstable vacuum*, Springer, (1991).
- [17] A. I. Nikishov, Problems of intense external-field intensity in quantum electrodynamics, *Journal of Russian Laser Research* **6**, 619 (1985).
- [18] T. Cheng, Q. Su and R. Grobe, *Phys. Rev. Lett.* **92**, 040406(2004); **93**, 043004 (2004); *Contemp. Phys.* **51**, 315 (2010); Q. Z. Lv, Y. Liu, Y. J. Li, R. Grobe, and Q. Su, *Phys. Rev. Lett.*, **111**, 183204 (2013).
- [19] F. Fillion-Gourdeau, E. Lorin, and A. D. Bandrauk, *Phys. Rev. Lett.* **110**, 013002 (2013); *J. Phys. B* **46**, 175002 (2013).
- [20] T. Zuo and A. D. Bandrauk, *Phys. Rev. A* **52**, R2511 (1995).
- [21] J. Wu, M. Meckel, L. Ph. H. Schmidt, M. Kunitski, S. Voss, H. Sann, H. Kim, T. Jahnke, A. Czasch and R. Dörner, *Nat Commun.* **3**, 1113 (2013).
- [22] H. Xu, F. He, D. Kielpinski, R.T. Sang and I.V. Litvinyuk, *Sci. Rep.* **5**, 13527 (2015).
- [23] S. Tang, B. S. Xie, D. Lu, H. Y. Wang, L. B. Fu, and J. Liu, *Phys. Rev. A* **88**, 012106 (2013).
- [24] G. R. Mocken and C. H. Keitel, *J. Comput. Phys.* **199**, 558 (2004); *Comput. Phys. Commun.* **178**, 868 (2008).
- [25] C. C. Gerry, Q. Su, and R. Grobe, *Phys. Rev. A* **74**, 044103 (2006).
- [26] Q. Wang, J. Liu and L. B. Fu, *Sci. Rep.* **6**, 25292 (2016).